

Physical properties of V_7O_{13} single crystals

B. F. Griffing,* S. A. Shivashankar,[†] S. Nagata,[‡] S. P. Faile,[§] and J. M. Honig
Department of Physics and Chemistry, Purdue University, West Lafayette, Indiana 47907

(Received 22 June 1981)

Heat capacity, resistivity, thermoelectric power, and magnetic susceptibility studies are reported for single crystals of V_7O_{13} obtained by chemical-vapor-transport techniques. The entropy change accompanying magnetic ordering effects at 43.5 K is well below the values calculated on the basis of charge differentiation. Electrical and susceptibility anomalies are in accord with theoretical predictions for the prevalence of antiferromagnetic order below 43.5 K. A change in sign of the Seebeck coefficient as well as sharply dropping resistivity with decreasing temperature below the Néel temperature suggests the presence of two bands at the Fermi energy.

I. INTRODUCTION

V_7O_{13} is a member of the homologous series V_nO_{2n-1} ($n > 3$), termed Magnéli phases, which lie between V_2O_3 and VO_2 in the vanadium-oxygen phase diagram. The V_nO_{2n-1} Magnéli phases are composed of VO_2 -like blocks, separated by crystallographic shear planes. At the shear plane, one VO_2 block is shifted with respect to the next and a layer of oxygen atoms is left out. The distance between shear planes varies with n , and provides the means by which the V/O ratio changes through the series. An alternative point of view is that the approximately hexagonally close packed oxygen lattice is fixed and that only the filling of octahedral centers with vanadium atoms varies with n . The average valence of the vanadium varies from $3d^2$ for V_2O_3 to $3d^1$ for VO_2 . In the Magnéli phases, the distribution of vanadium atoms in the lattice is nonuniform. The average vanadium density is higher at the shear planes than between shear planes.

Most of the Magnéli phases display a metal-insulator transition at higher temperatures as well as an antiferromagnetic transition at lower temperatures.¹ V_7O_{13} differs from the rest in that no metal-insulator transition takes place in the range 1.2–1100 K.¹ The compound nevertheless undergoes a magnetic ordering transition near 43 K.¹

In agreement with earlier workers² we observed a very large linear contribution to the low-temperature specific heat. If this term is attributed to electronic degrees of freedom, then it corresponds to a density of states at the Fermi energy of 17/eV vanadium and the Fermi level would then intersect the V $3d$ band. On the other hand, NMR and magnetic susceptibility measurements provide evidence for localized moments in the high-temperature (HT) phase. These localized moments would normally be associated with the V $3d$ electrons; however, a difficulty arises because, as noted above, $3d$ states occur at the Fermi

level. In rare-earth metals this problem is resolved because the local and itinerant properties are due to the f and s electrons, respectively. An analogous s - d assignment for the vanadium oxides runs into problems. Band-structure calculations³⁻⁸ for the end members of the series (VO_2 and V_2O_3), as well as experimental evidence indicate that the V $4s$ levels are energetically well separated from the d states. NMR experiments on V_7O_{13} (Refs. 9 and 10) show that the fractional s character of electrons at the Fermi level is quite small, if not zero. We suggest this problem can be resolved by attributing both the localized and itinerant properties to the V $3d$ electrons. While the coexistence of localized and itinerant d electrons in oxides is not a new concept,¹¹ it was not clear whether or not this idea could be applied to V_7O_{13} .

II. EXPERIMENTAL

A. Sample preparation

The V_7O_{13} crystal was prepared in the Purdue Central Materials Preparation Facility following the procedure specified by Nagasawa *et al.*¹² The batch which was ultimately found to contain the single "good" V_7O_{13} platelet was originally intended to be V_6O_{11} instead of V_7O_{13} . The low-temperature specific heat of this whole batch was measured by Khattak *et al.*¹³ and designated by them as sample V_6O_{11} (B). They concluded that this sample was not representative of pure V_6O_{11} due to the large linear term present at low temperature, which they attributed to impurities. Later investigation showed that this sample actually was mixture containing approximately 20 mole % V_7O_{13} , 4 mole % V_8O_{15} , and 76 mole % V_6O_{11} . Several of the platelets were found to be mixtures of two adjacent phases, as determined by specific heat and susceptibility experiments done on individual pieces. One platelet was identified that showed no

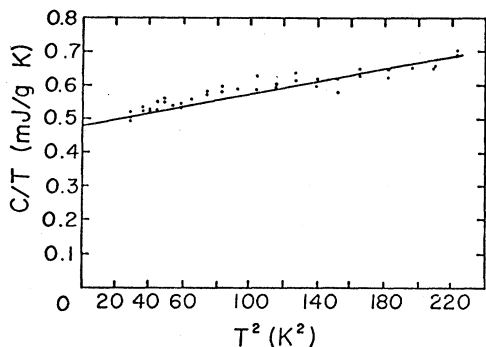


FIG. 1. Plot used to determine the linear contribution to the specific heat of V_7O_{13} .

evidence of any phases other than V_7O_{13} in susceptibility, specific heat, and resistivity measurements. All of the experiments reported here were made on pieces of this 90-mg platelet.

B. Specific heat

Specific heat (C) measurements in the temperature (T) range of 4–380 K were carried out using a relaxation calorimeter; the experimental details have been described elsewhere.¹⁴ A plot of C/T vs T^2 in the 0–16-K temperature range is shown in Fig. 1. The linear term in the specific heat, as determined by this plot, has a value of 4.8×10^{-4} J/g K². This is in reasonable agreement with the result of McWhan *et al.*² who reported a value of 4.2×10^{-4} J/g K² for a powdered sample embedded in copper dust. To within our limits of accuracy,¹⁵ we do not observe the

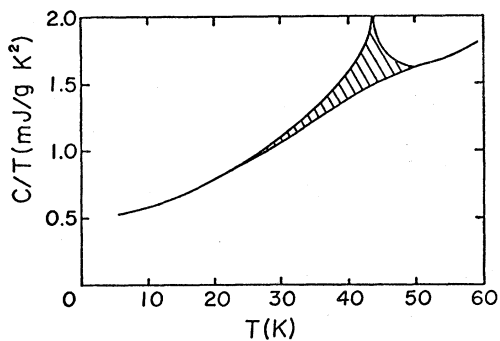


FIG. 2. Plot used to determine ΔS_N , the entropy change associated with the Néel transition at 43.5 K.

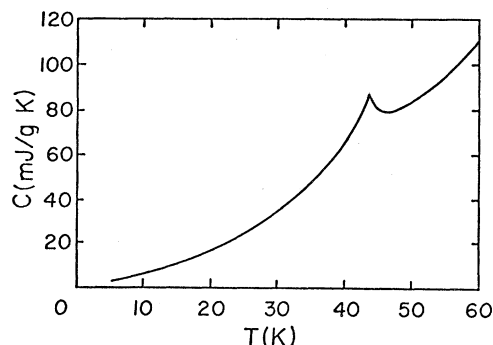


FIG. 3. Specific heat of V_7O_{13} in the 0–60-K range.

“extra” peak at 9 K which McWhan and co-workers attributed to impurities.¹⁶ Figure 2 is the plot of C/T vs T used to compute the entropy change ΔS_N , associated with the Néel transition at 43.5 K. Due to the large linear term in the specific heat, it is difficult to provide an accurate estimate of ΔS_N . While the calculated ΔS_N , 1.9 J/K mole V_7O_{13} , may be slightly low, no reinterpretation of the data could be made to obtain a result even moderately close to the value calculated on the basis of complete charge differentiation:

$$\Delta S_N = R(2 \ln 3 + 5 \ln 2) = 47 \text{ J/K mole } V_7O_{13} \quad (1)$$

The specific heat versus temperature is plotted in Figs. 3 and 4 in the 5–380-K range to illustrate the absence of features at all measured temperatures, other than the magnetic ordering at 43.5 K. This suggests that the sample is relatively free of contamination from adjacent Magnéli phases.

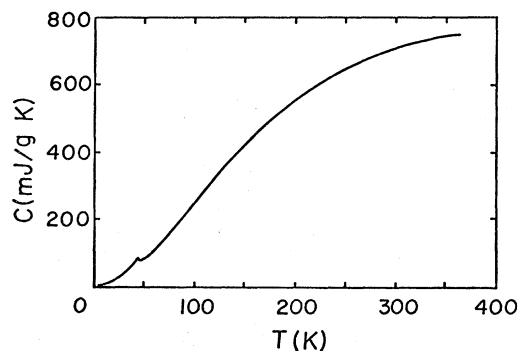


FIG. 4. Specific heat of V_7O_{13} in the 0–400-K range.

C. Resistivity

Resistivity measurements were carried out using the standard four-probe technique in a dip-tube cryostat. The results shown in Fig. 5 represent data taken along three mutually perpendicular directions. The curves marked A and B represent measurements taken in the plane of the platelet sample, while curve C corresponds to current flow perpendicular to this plane. X-ray orientations have not been carried out, but it is known¹⁷ that the direction perpendicular to the plane of the platelet is usually the crystallographic c direction as defined by Horiuchi *et al.*¹⁸ The geometric factors are known to within an accuracy of only about 30%, so that the relative positions of curves A and B may be reversed, but it is relatively certain that both A and B lie below C. The temperature dependence of $(1/\rho)$ ($d\rho/dT$) near the critical temperature for sample C is shown in Fig. 6. This critical behavior, as well as the rapid reduction of the resistivity with decreasing temperature below 30 K was not reported by previous investigators.¹ This difference in observations might be due to the relatively larger residual resistivity caused by impurities and defects in previous samples. In this case we refer to actual impurities and not adjacent Magnéli phases. This conjecture is supported by the much lower resistivity at 4.2 K in our samples, and by the susceptibility measurements discussed below.

The resistivity variation near the critical temperature for both ferromagnetic and antiferromagnetic systems has been discussed in the literature.¹⁹⁻²¹ The predictions made for the two cases differ in the sign of $(1/\rho)$ ($d\rho/dT$) at the critical temperature. Previous Mössbauer experiments^{1,22} provided evidence that the transition at 43.5 K in V_7O_{13} is magnetic in origin. The temperature dependence of the susceptibility yielded a negative value of the Weiss constant θ which is taken as an indication of antiferromagnetism. The observed minimum in $(1/\rho)$ ($d\rho/dT$)

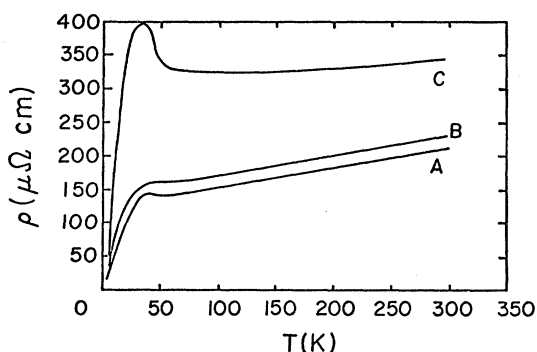


FIG. 5. Resistivity of V_7O_{13} in three mutually perpendicular directions. A and B lie in the plane of the as-grown single crystal platelet; C is perpendicular to this plane.

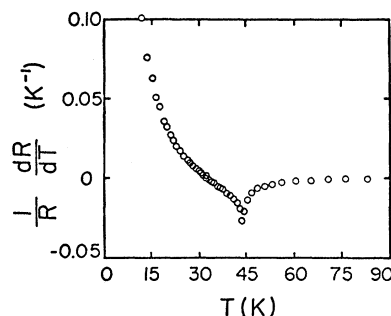


FIG. 6. Normalized temperature derivative of resistivity in the critical temperature range, along direction c . Presence of a minimum indicates antiferromagnetic ordering.

which occurs at the same temperature as the specific-heat peak is in agreement with the theoretical prediction²¹ for antiferromagnetic ordering and provides additional evidence for the antiferromagnetic nature of the transition.

D. Magnetic susceptibility

Susceptibility measurements were carried out in the 4–120-K range using a SQUID apparatus which has been described elsewhere.²³ Several pieces of the original sample with a total mass of 35 mg, were used: their orientations were random. The susceptibility versus temperature of V_7O_{13} in an applied field of 15 Oe is shown in Fig. 7. Below 90 K the data are very accurate but above 90 K only an extrapolation of the temperature calibration was used, so that the temperature scale is less accurate. The susceptibility between 55 and 90 K can be expressed by the Curie-Weiss form: $\chi = C/(T - \Theta) + \chi_0$ with $C = 0.48$ (emu K/mole V), $\Theta = -45$ K, and $\chi_0 = 8.1 \times 10^{-4}$ (emu/mole V). From this value of C , and using 2 for the Landé g factor, follows the effective number of Bohr magnetons: $P_{\text{eff}} = 1.96$. These results are of the same order as for previous data.¹ The calculated values of C and P_{eff} for two V^{3+} and V^{4+} ions per formula unit are 0.554 and 2.104, respectively, so that a simple localized model of vanadium ions would indicate that 87% of the ions are localized. Assuming Pauli paramagnetism for χ_0 the density of states at the Fermi level per vanadium ion is estimated to be 25/eV vanadium. This value is slightly larger than that obtained from the large linear term γ of the specific heat mentioned above, 17/eV vanadium.

Below 43 K, the Néel temperature, the results are qualitatively different from those obtained by previous investigators.^{1,9} The susceptibility below 38 K is independent of temperature and does not tend to increase at low temperatures, as previously reported.⁹ The usual explanation for such a rise at low temperatures involves the presence of isolated magnetic impurities, which exhibit a Curie-like susceptibility.

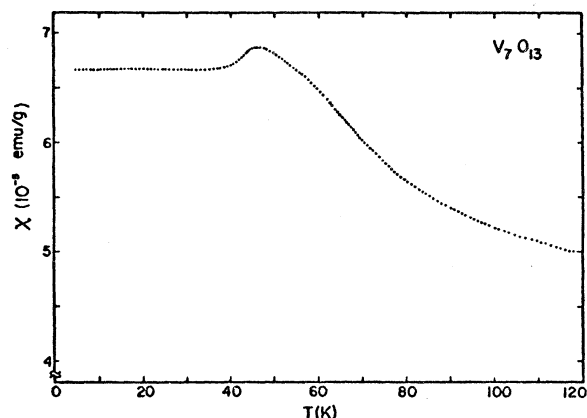


FIG. 7. Susceptibility of V_7O_{13} in the 0–120-K range.

The qualitative differences between the susceptibility and resistivity reported here and those of previous workers may be attributed to the relatively higher quality of our crystals.

For the localized moment model, the constant susceptibility below 38 K can be understood if the crystal is antiferromagnetic with a very low anisotropy field. In that case the magnetic moments are always perpendicular to the applied magnetic field, so that the measured susceptibility is χ_{\perp} , which is constant below the Néel temperature. The molecular-field approximation yields $\chi_{\perp} = N(g\mu_B)^2/4z|J|$, where $g = 2$, N is

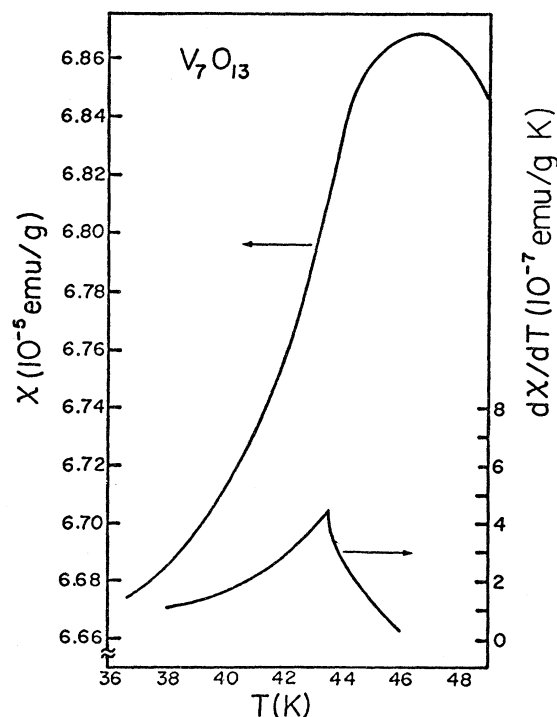


FIG. 8. Susceptibility and temperature derivative of susceptibility in the critical temperature range.

the number of magnetic ions, z is the number of nearest neighbors, and μ_B is the Bohr magneton. It then follows for the effective exchange constant that $zJ/k = -69$ K. A comparable value of the exchange constant ($zJ/k = -61$ K) follows also from the Weiss constant using the relation $\Theta = 2zJS(S+1)/3k$, where $S(S+1)$ is the value of 1.11 calculated from the chemical formula.

Figure 8 contains a plot of susceptibility versus temperature and $d\chi/dT$ versus temperature in the critical temperature range. The temperature dependence of $d\chi/dT$ is similar to the temperature dependence of the specific heat in this region. Both variations are in accord with the predictions of Fisher²⁴ for an antiferromagnetic system of completely localized moments.

E. Seebeck coefficient

The Seebeck coefficient for a metal depends sensitively on the electronic structure of the metal (the Fermi surface) and on the manner in which conduction electrons are scattered when temperature gradients are present. The interpretation of Seebeck measurements is more obtuse than that of thermal and electrical conductivities. However, such measurements can be a valuable addition to other data in understanding the band structure of a metal.

Measurements of the Seebeck coefficient (α) of V_7O_{13} in the temperature range 30–200 K were carried out in the same dip-tube cryostat as used for resistivity measurements. The heat winding on the top end of the copper sample block, previously used for feedback temperature regulation, was used to establish the temperature gradient (ΔT) that generates the Seebeck voltage (ΔV). ΔT was measured by two copper-Constantan thermocouples indium-soldered to the two ends of the sample, mounted so that the applied gradient is parallel to the natural temperature gradient in the cryostat. The (mean) temperature of the sample was measured by a calibrated silicon diode.

The processing of the ΔT and ΔV signals was done using an electronic circuit patterned after the one described by Keem and Honig.²⁵ The differential temperature signal was obtained by subtracting the thermocouple voltages in an analog subtractor constructed with low-noise operational amplifiers.²⁶ The Seebeck voltage was measured across the sample with its colder end grounded. Both the ΔT and ΔV signals were amplified and filtered in closely matched low-pass continuous averaging filters. The filtered ΔT and ΔV signals were fed into the X and Y axis, respectively, of an XY recorder.

To measure the Seebeck coefficient α , the sample temperature was allowed to stabilize at a desired value; power was then applied to the heater. As a temperature gradient develops and subsequently re-

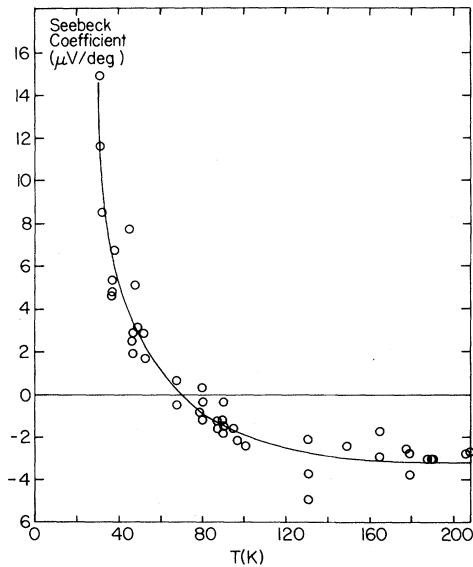


FIG. 9. Seebeck coefficient of V_7O_{13} in 0–300-K range.

laxes, the XY recorder traces a narrow loop. (If the filters in the ΔT and ΔV arms were matched perfectly, the loop would be of zero width, i.e., a straight line would be obtained.) For small applied gradients, α is given by the slope of the straight line joining the two ends of the loop.

Seebeck coefficients versus temperature for V_7O_{13} are shown in Fig. 9. The sample used was the one designated A in Fig. 5, i.e., cut parallel to the plane of the grown platelet. Anisotropy in α could not be measured because of the very small dimensions of sample C. The results shown are at variance with those of Okinaka *et al.*²⁷ who reported $\alpha \approx -10 \mu V/K$ in the measured range of 110–300 K. Our measurements show that α changes from positive to negative at about 50 K ($T_N = 43.5$ K). The temperature at which this change of sign occurs is rendered somewhat uncertain due to the use of copper leads in measuring the Seebeck voltage, because the phonon drag effects leads to a peak in the Seebeck coefficient of copper at about 50 K.²⁸ Measurements could not be made below ~ 35 K, both because the thermocouple used lost their sensitivity and because the cryostat design was not suited for such low temperatures.

III. DISCUSSION

The band structure of oxides is often discussed in terms of the tight binding approximation. In V_7O_{13} , the V cations are in sites which are roughly octahedrally coordinated by oxygen anions. The five degenerate atomic $3d$ levels are shifted and split by an octahedral crystal field into t_{2g} and e_g levels, which then broaden into bands. Distortions from the

octahedral site symmetry further split the degenerate atomic $3d$ levels, which subsequently form bands. This approach correctly predicts the metallic nature of V_7O_{13} , but fails to provide a mechanism for the observed localized moments. Others^{2,9,10} have suggested that there is presently no theory to account for either the metal-insulator transitions or the localized moments (in the metallic state) of the V Magnéli phases. NMR studies of the metallic state^{9,10} of several Magnéli phases provide evidence for charge localization at least on the microsecond time scale. The susceptibility above T_N has previously been discussed^{1,9} in terms of complete charge localization and Curie-Weiss behavior. Our susceptibility data also support the predominantly localized ($\sim 87\%$) d electron picture. Nevertheless a serious discrepancy exists between this localized moment model and the results of the specific heat, as the magnetic entropy change (ΔS_N) is extremely small when compared to that expected for localized moments. From the magnetic point of view the metallic states for all the Magnéli phases have common features and appear to exhibit well-localized magnetic moments with strongly temperature dependent susceptibility. However, our experimental results for V_7O_{13} indicate that the localized magnetic behavior does not imply a large magnetic entropy. Stated differently, the susceptibility data fit well to a completely localized moment model with 87% of the sites participating, while the entropy of transition suggests that only 4% of the sites are magnetically active. NMR^{9,10} experiments show no evidence for singlet pairs states, which might otherwise explain the discrepancy. The large density of states at the Fermi energy, as measured by both specific and susceptibility, suggests the presence of a narrow d band. That this single band could be responsible for the observed Seebeck coefficient, low-temperature electrical conductivity, large γ , and localized moments seems unlikely. Indeed, the change in sign of the Seebeck coefficient suggests the possibility that at least two bands intersect the Fermi energy. Since no structural changes occur over the temperature range in which these effects occur, the reversal is most probably due to changes in electron scattering, rather than band structure (effective mass) shifts. Because this apparent shift in scattering occurs near the antiferromagnetic ordering temperature, the scattering mechanism is most probably magnetic in origin. While the picture of two or more bands at the Fermi energy seems to fit most of the experimental data, the question of entropy in the Néel transition is left open in this picture, due to lack of a theoretical model describing such a system. The coexistence of d electrons in both itinerant and localized states at the Fermi energy represents a case which is not treated by conventional band theories. A quantitative understanding of these data awaits further theoretical work.

ACKNOWLEDGMENTS

The authors are greatly indebted to Professor P. H. Keesom and Professor L. L. Van Zandt for many stimulating discussions. Research supported by NSF Grant No. DMR79-80356.

- *Permanent address: General Electric Company, Research and Development Center, Schenectady, N.Y. 12309.
 † Present address: IBM Watson Research Center, P. O. Box 218, Yorktown Heights, N.Y. 10598.
 ‡ Present address: Ames Laboratory—USDOE and Department of Physics, Iowa State University, Ames, Iowa 50011.
 § Permanent address: General Electric Company, Aircraft Engine Group, Cincinnati, Ohio 45215.
- ¹S. Kachi, K. Kosuge, and H. Okinaka, *J. Solid State Chem.* **6**, 258 (1973).
²D. B. McWhan, J. P. Remeika, J. P. Maita, H. Okinaka, K. Kosuge, and S. Kachi, *Phys. Rev. B* **7**, 326 (1973).
³E. Caruthers, L. Kleinman, and H. I. Zhang, *Phys. Rev. B* **7**, 3753 (1973).
⁴E. Caruthers and L. Kleinman, *Phys. Rev. B* **7**, 3760 (1973).
⁵M. Gupta, A. J. Freeman, and D. E. Ellis, *Phys. Rev. B* **16**, 3338 (1977).
⁶J. Ashkenazi and T. Chuchem, *Philos. Mag.* **33**, 763 (1975).
⁷J. Ashkenazi and M. Weger, *Adv. Phys.* **22**, 207 (1973); *J. Phys. (Paris)* **37**, C4-189 (1976).
⁸C. Castellani, C. R. Natoli, and J. Ranninger, *Phys. Rev. B* **18**, 4945, 4967, 5001 (1978).
⁹A. C. Gossard, J. P. Remeika, T. M. Rice, H. Yasuoka, K. Kosuge, and S. Kachi, *Phys. Rev. B* **10**, 4178 (1974).
¹⁰A. C. Gossard, F. J. DiSalvo, L. C. Erich, J. P. Remeika, H. Yasuoka, K. Kosuge, and S. Kachi, *Phys. Rev. B* **10**, 4178 (1974).
¹¹J. B. Goodenough, *Mater. Res. Bull.* **6**, 967 (1971).
¹²K. Nagasawa, Y. Bando, and T. Takada, *Jpn. J. Appl. Phys.* **8**, 1262 (1968).
¹³G. D. Khattak, P. H. Keesom, and S. P. Faile, *Phys. Rev. B* **18**, 6181 (1978).
¹⁴B. F. Griffing and S. A. Shivashankar, *Rev. Sci. Instrum.* **51**, 1030 (1980); B. F. Griffing, Ph. D. thesis (Purdue University, 1979) (unpublished).
¹⁵Due to the diode temperature sensor, our calorimeter is least accurate (5%) at the lowest temperatures (5 K in this case). The accuracy increases with increasing temperature up to about 30 K (2%), beyond which it is approximately constant.
- ¹⁶McWhan *et al.* observed an extra peak in the specific heat of each of their metallic samples which they attributed to impurities. We would like to provide an alternative interpretation of these peaks. Our experience indicates that the most common "impurity" to a Magnéli phase sample is an adjacent Magnéli phase. For example, a small concentration of V_8O_{15} in a V_7O_{13} sample is very hard to detect using x rays, and may only be detected in a specific heat or susceptibility measurement. Such a V_8O_{15} "impurity" in the V_7O_{13} sample of McWhan *et al.* would provide the extra peak at just the right temperature due to magnetic ordering. The bump seen in their $V_{1.97}O_3$ data is probably due to the recently reported (Ref. 28) magnetic ordering in this material at 9 K. The peak in the $V_{0.82}W_{0.18}O_2$ data is not understood, but it may also be due to magnetic ordering effects.
- ¹⁷H. Sato (personal communication).
¹⁸H. Horiuchi, N. Morimoto, and M. Tokonami, *J. Solid State Chem.* **17**, 407 (1976).
¹⁹M. Fisher and J. Langer, *Phys. Rev. Lett.* **20**, 665 (1968).
²⁰H. Mori and H. Okamoto, *Prog. Theor. Phys.* **40**, 1287 (1968).
²¹Y. Suezaki and H. Mori, *Prog. Theor. Phys.* **41**, 4177 (1969).
²²H. Okinaka, K. Kosuge, S. Kachi, M. Takano, and T. Takada, *J. Phys. Soc. Jpn.* **32**, 1148 (1972).
²³Except for the fact that the absolute accuracy of the system has been improved, the experimental details of the SQUID apparatus are described in S. Nagata, P. H. Keesom, and H. R. Harrison, *Phys. Rev. B* **19**, 1633 (1979).
²⁴M. Fisher, *Philos. Mag.* **7**, 1731 (1962).
²⁵J. E. Keem and J. M. Honig, *Phys. Status Solidi (B)* **28**, 335 (1975).
²⁶The amplifiers used were AD517J and AD517K, manufactured by Analog Devices, Inc.
²⁷H. Okinaka, K. Nagasawa, K. Kosuge, Y. Bando, S. Kachi, and T. Takada, *J. Phys. Soc. Jpn.* **29**, 245 (1970).
²⁸D. K. C. Macdonald, *Thermoelectricity: An Introduction to the Principles* (Wiley, New York, 1962).